IJSGS

ISSN: 2488-9229
FEDERAL UNIVERSITY
GUSAU-NIGERIA

INTERNATIONAL JOURNAL OF SCIENCE FOR GLOBAL SUSTAINABILITY

Identification of Lineaments within Gitata Using Derivative, Euler Deconvolution and Centre for Exploration Targeting CET

***Mam D. Tawey[1*], Emmanuel E. Udensi[2], Abbass A. Adetona[2] Usman D. Alhassan[2]**
[1]National Water Resources Institute, Mando Road Kaduna
[2]Geophysics Department Federal University of Technology Minna

Corresponding Authors email: taweymam@gmail.com **Phone no:** 08065678908

Received on: November 2017 **Revised and Accepted on:** September 2019

ABSTRACT

A digitised aeromagnetic data was acquired and analysed to delineate geological lineaments and depths to the magnetic bodies within Gitata sheet (187) covering approximately an area of 55×55km^2 bounded by latitude 9 ^{0} N to 9^0 30^1 N and Longitude 7 ^{0} 30 ^{1} E to 8 ^{0} E in north central Nigeria within part of Federal Capital Territory, Kaduna and Nasarrawa state using High-Resolution Aeromagnetic Data (HRAD). First vertical derivative, 3D Euler deconvolution and the CET grid analysis of the acquired aeromagnetic data using Oasis Montaj and other geologic information within this area were employed in the structural classification. The HRAD was processed to identify anomalies of concern and findings of the HRAD's first vertical derivative and CETmaps revealed that the research area is highly faulted. From 3D Euler deconvolution, depths were divided and grouped at every 150 m and the result shows that the faults / fractures between the depths of 150 and 300 m dominate the study area. The outcome also demonstrates the prominent trending NE–SW and NW–SE structures. A critical visual inspection of the fault pattern indicated by the NE–SW trend alignment of many Euler solutions indicates that the study area has been seriously influenced by the NE–SW trend of the regional fault system.

Key words: Structures, Aeromagnetic, Deconvolution and CET

1.0 INTRODUCTION

The importance of geological structures cannot be overstated in geology / hydrogeology / geophysics, civil engineering and building engineering. Structures generally play a very important role in our day-to-day activities, be it in groundwater exploration as these structures are conduit for water especially in the basement complex where the overburdened thickness of the sediment is thin, in mineral exploration, these structures serve as host to most of the minerals.

In dam construction as the presence of these structures within dam axis can lead to failure also, in road construction and even in building where it is built on a weak structure below, it may fail which will lead to lead to loss of lives and properties as the case may be.

Magnetic method is considered to be one of the most effective and suitable tools that promote the identification of these geological structures and magnetic assessment can be used in the mapping of regional structural zones, dike-like structures, deep contact, rock differentiation locations, sedimentary depth and mineralization (Domzalski, 1966). The magnetic method does have the advantage that it is a quick and efficient technique for studying the geological structure of the subsurface and mapping the fractured basement. (Azizi*et al.*, 2015; Farhi*et al.*, 2016; and Khashaba*et al.*, 2016). The function of aeromagnetic method in mineral exploration differs from delineation of structures such as faults, folds, contacts, shear zones and intrusions into automated porphyry detection and favorable mineral deposit areas. As such, the present work is directed at identifying and delineating the lineaments within the study area that could address the issue of the application of the structures listed above.

1.1 Location of Study Area

The area of study falls within two states and the federal capital territory. These are Kaduna and Nasarrawa states (Figure 1). It is bounded by latitude 9 ^{0} N to 9 ^{0} 30^{1} N and Longitude 7 ^{0} 30^{1} E to 8^{0}E.The study area falls within the north central Nigerian basement complex and extend from south of Abuja to east of UngwarAlura in the south and from north of Kwoi town to west of Kajuru in the north.

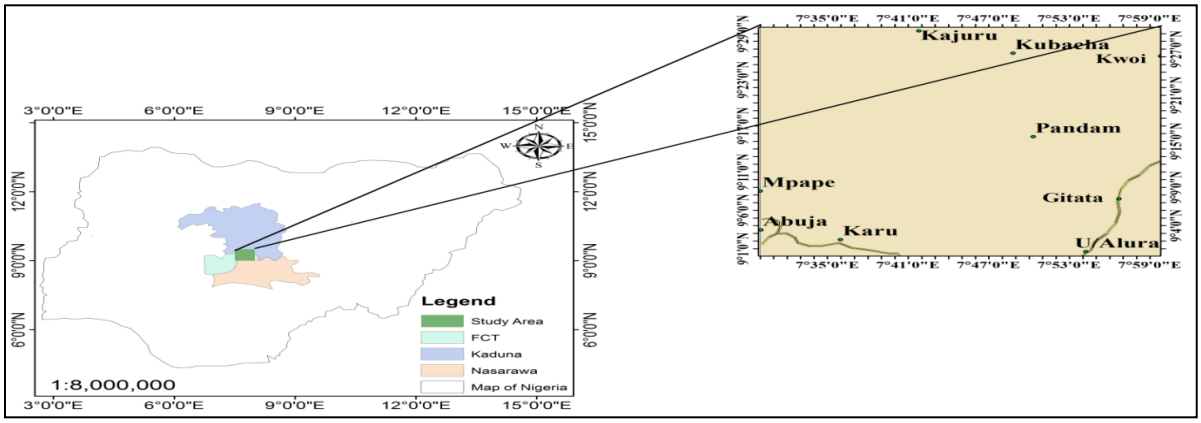

Figure 1 Location of study area on Nigerian map

1.2 Geology of the Area

The basement complex is one of the three major litho-petrological components that make up the geology of Nigeria. The Nigerian basement complex forms a part of the Pan-African mobile belt and lies between the West African and Congo Craton and south of the Tuareg Shield (Black, 1980). It is intruded by the Mesozoic calc-alkaline ring complexes (Younger Granites) of the Jos Plateau and is unconformably overlain by Cretaceous and younger sediments. Within the basement complex of Nigeria four major petro-lithological units:

a. The Migmatite – Gneiss Complex (MGC) b. The Schist Belt (Metasedimentary and Metavolcanic rocks) c. The Older Granites (Pan African granitoids) and d. Undeformed Acid and Basic Dykes. Migmatite is the most abundant rock type in this area (Figure 2) with other occurrence of Biotite Granite, Medium to Coarse Grained Biotite Granite, Muscovite and Quartz Muscovite Schist, Porphyroblastic Older Granite and Undifferentiated Schist and Gneiss.

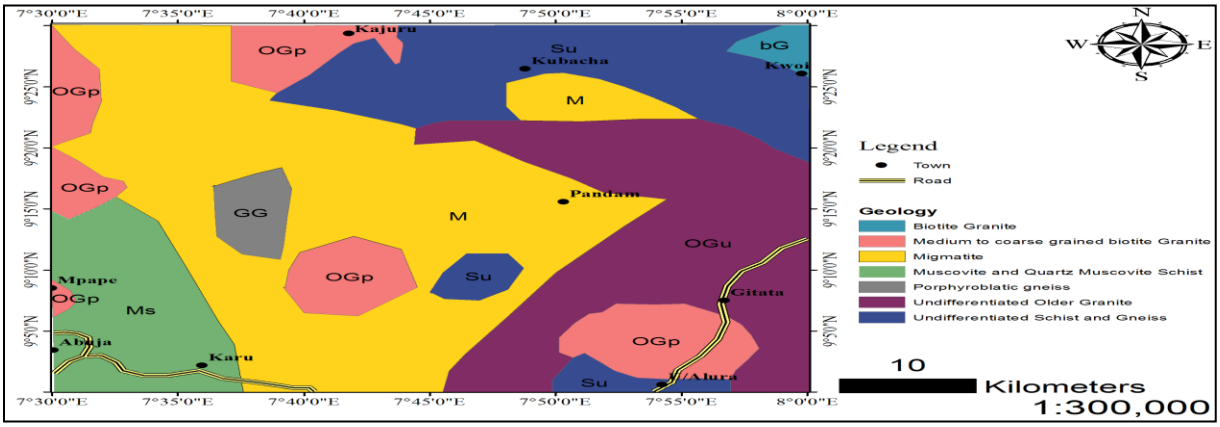

Figure: 2. Geologic Map of the Area (NGSA, 2006) Modified

2.0 MATERIAL AND METHODS

2.1 Source of Aeromagnetic Data

The aeromagnetic data sheet (187, Gitata) used for this research was acquired from the Nigerian

Geological Survey Agency (NGSA) Abuja. The survey was conducted between 2005 and 2009 and it was funded by the Federal Government of Nigeria and the World Bank. The survey took place in two phases. Phase 1 was financed fully by the Government of Nigeria, while phase 2 was financed by both the Government of Nigeria and the World Bank. Fugro Airborne Surveys conducted all acquisition, processing and analysis of airborne geophysical data.

2.2 Methodology

The methods involved in this study include:

1. Production of Total Magnetic Intensity (TMI) map of the study area reduced to magnetic equator in color aggregate using Oasis Montaj software
2. Application of First Vertical Derivative to manually map out the structures
3. Application of Centre for Exploration Targeting Plug-IN (CET) for Automatic structural extraction
4. Produce Euler deconvolution map for structures and depth to magnetic source bodies

2.3 Reduction to Magnetic Equator (RTE)

Contrary to the case of gravity in which anomalies are generally above the source that produces them, the magnetic anomalies observed in the low and middle latitudes show a polarity that complicates their interpretation. This shape of magnetic anomalies is caused by the inclination of the induced field vector and the magnetisation vector (Yaoguo and Douglas, 2001). To counter this "skewness," Baranov (1957) introduced a transformation procedure called Pole Reduction (RTP) that allows magnetic anomalies to be repositioned above the causative source.

However, as the magnetic latitude approaches the equator, the (RTP) operator is unbound along the direction of magnetic declination and therefore amplifies the noise in this direction to the extent that the resulting (RTP) field is dominated by linear features aligned with the direction of declination. The horizontal inductive field at the equator causes the pattern of the induced magnetic anomaly to be highly dependent on its orientation. The same east-west-oriented body may generate a large anomaly eventually; the long north-south-oriented bodies may be almost invisible magnetically, even if the magnetic body has a high magnetic susceptibility. The Reduce-to-Equator (RTE) filter was introduced and applied to the total magnetic intensity data to transform the data into its equatorial pattern, after which the data was multiplied by the appropriate parameters to mimic the anomaly magnitude as it would appear in the equator. The stability of the RTE filter enabled the filtered result to appear undistorted. As a result, the regional magnetic field and the source magnetic field are horizontal.

2.4 Vertical Derivative

Vertical derivative (or alternatively named vertical gradient) filters preferentially amplify short-wavelength components of the field at the expense of longer wavelengths (Foss, 2011). Vertical derivative filters are generally applied to gridded data using FFT (Fast Fourier Transform) filters. Various vertical derivatives of the magnetic field can be computed by multiplying the amplitude spectra of the field by a factor of the form:

$$\frac{1}{n}\left[(U^2+V^2)^{\frac{1}{2}}\right]^n \qquad 1$$

Where n is the order of the vertical derivative, (U, V) is the wavenumber corresponding to the (x, y) directions respectively. The first vertical derivative is physically equivalent to measuring the magnetic field simultaneously at two points vertically above each other, subtracting the data and dividing the result by the vertical spatial separation of the measurement points. Since derivatives tend to sharpen the edges of anomalies and enhance shallow features, it was applied to the data and the structures manually mapped out.

2.5 Centre for Exploration Targeting Grid Analysis.

The Center for Exploration Targeting (CET) is a suite of algorithms that offers functionality for improvement, lineament detection and structural complexity analysis of potential field data

(Holden *et al*., 2008; Core *et al*., 2009). This method automatically delineates lineaments and selects promising areas of ore deposits through outlining convergence regions and also the divergence of structural components through a number of statistical steps, including texture analysis, lineation delineation and vectorisation.

2.5 Texture Analysis

Texture analysis characterises the local area of each image location. Discontinuity areas aretherefore areas with high standard deviation values. Alternatively, the entropy filter had also been realised to be efficient in the improvement and enhancement of local anomalies.

2.6 Texture Ridge Detection

Texture ridge detection was used to locate laterally continuous ridges within the texture analysis output. Ridge characteristics are identified by a contrast invariant line-like feature detection method based on local phase symmetry. This method enables the detection of all ridges, regardless of their image contrast to the environment.

2.7 Thinning of Texture Ridges

Line segment Vectorisation analyses the texture ridges identified by phase symmetry and finds line segments representative of the ridges. This is achieved by thresholding the output of the phase symmetry to generate a binary grid (i.e. black and white) that specifies the foreground texture ridges as white and the background as black. The binary grid was then processed to produce axial rows of texture ridges by thinning / skeletonisation. Next, the skeletal structures wereanalysed to create a collection of straight-line sections that best match the skeletal structure.

2.8 3D Euler Deconvolution

Most of the processing algorithms proposed for the analysis of magnetic data either estimate the depth or find the boundary. However, Euler deconvolution is both a border and a depth estimator (Reid et *al*., 1990). It extracts data from grids using the homogeneity relationship shown by (Thompson, 1982). This relationship can be written in the following form:

$$(x - x_0)\frac{\delta T}{\delta x} + (y - y_0)\frac{\delta T}{\delta y} + (z - z_0)\frac{\delta T}{\delta z} = N(B - T) \quad 2$$

where$(x_0, y_0, z_0)$is the position of a magnetic source whose total field T is detected at (x, y, z). B is the regional field value; and N is the degree of homogeneity interpreted as the structural index (SI) (Thompson, 1982), which is a measure of the rate of change at field distance, and this structural index was chosen on the basis of prior knowledge of the source geometry. Structural index (SI) ranges from zero (0) to three (3) for distinct bodies (N= 0 for contacts, 1 for sill / dyke / fault, 2 for pipe / horizontal bodies, and 3 for spherical bodies) (Reid *et al.,* 1990).

3.0 RESULTS AND DISCUSSIONS

3.1 TMI Map and TMI Reduced to Magnetic Equator Map

The total magnetic intensity map (Figure 3) shows the variation in magnetic intensity of anomalies across the study area from south to north and from east to west. The map (Figure 3) shows some positive (red) and negative (deep blue) anomalies. These Positive (red-colored) anomalies are observed around the south-eastern part of the map and there are also isolated occurrences of positive (red-colored) anomalies in the north-western end having both NE-SW and NW-SE trends. Negative (deep blue) anomaly is observed in the central portion of the map (Figure 3) with a north-east to south-west orientation. There are also isolated occurrences of negative (deep blue coloured) anomalies having trend of NE-SW around the north eastern part of the map. Figure 4 is the TMI map reduced to magnetic equator. This map has both the positive (red coloured) and negative (deep blue coloured) anomalies having orientation and trend just like the TMI map but a closer look at the maps reveals differences in sizes of the anomalies in both maps especially the positive (red coloured) directly above the negative (deep blue coloured) anomaly in TMI map has now greatly reduced in size in TMI reduce to equator map Figure 4. Figure 5 is the residual map of the area. Here, anomalies are having both north-east to south-west and north-west to south-east trend.

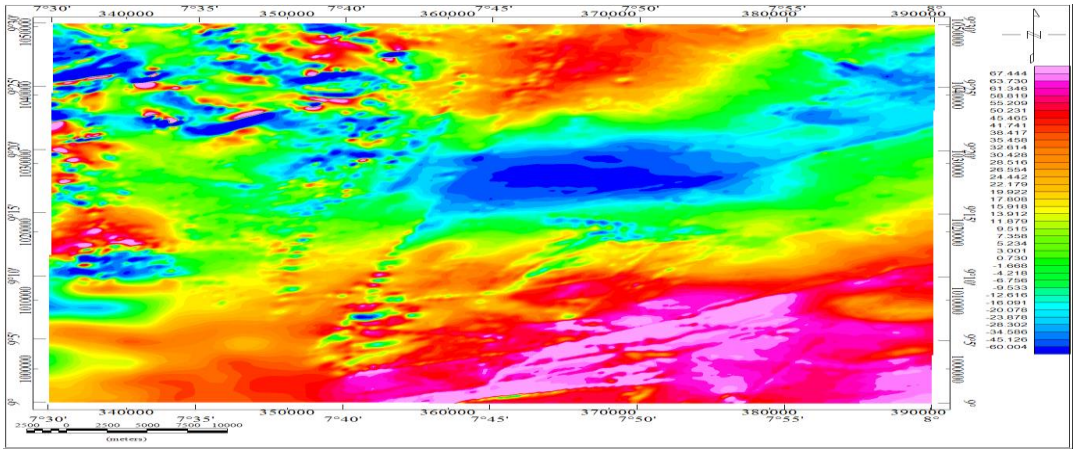

Figure: 3. Total Magnetic Intensity Map (nT)

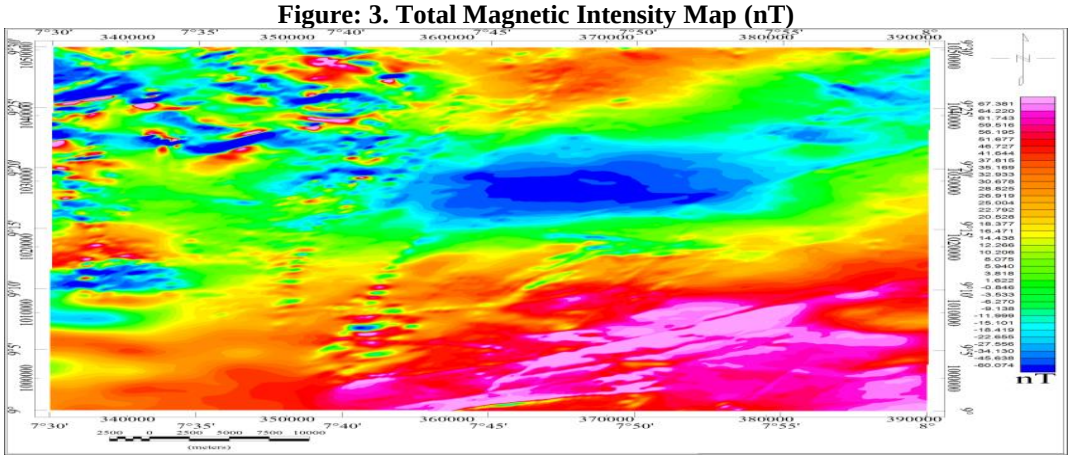

Figure: 4. Total Magnetic Intensity Reduced to Equator Map

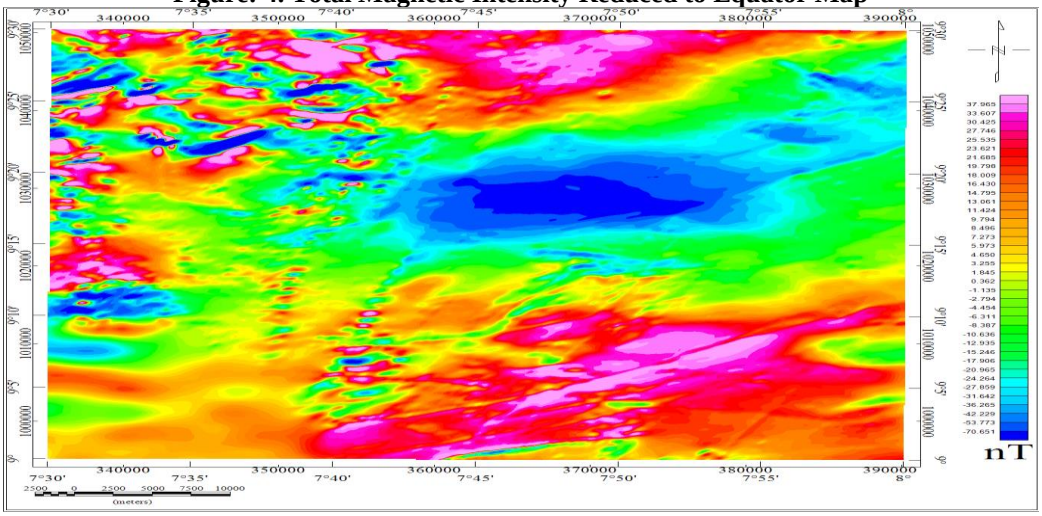

Figure: 5. Residual Map of the area

3.2 Derivative Map

The vertical derivative map (Figure. 6) provides an excellent representation of near-surface features such as faults (Black lines) where the filter enhances short-wavelength anomalies responsible for shallow sources at the expense of long ones. It is noticeable here that the research area is a highly faulted region and is occupied by such short-wavelength anomalies indicating a relatively shallow depth of the causative source.

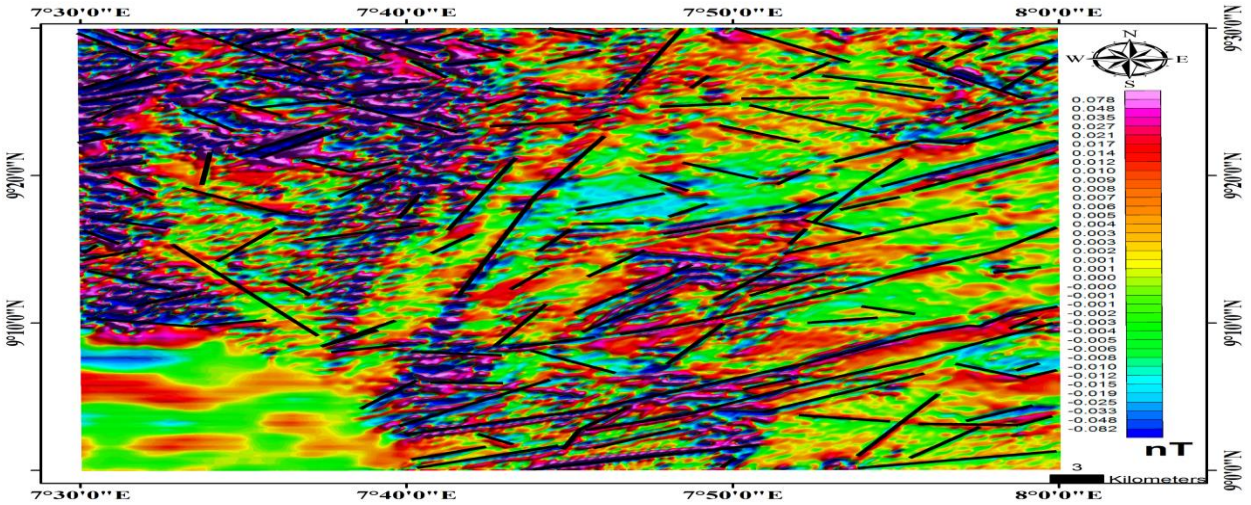

Figure: 6. First Vertical Derivative Map with Lineaments in Black

3.3 CET Analysis Maps

Standard deviation map (Figure.7) displays the output that reflects the spread of variations in the magnetic intensity of the study area. As a result, discontinuity zones are areas that show more variability and display high standard deviation values. The sections identified are linked to both structural and lithological limits. The output of the phase symmetry (Figure. 8) was calculated from the image shown in (Figure.7). It shows the local structure in the image that enables the ridges as well as the valleys to be detected. Symmetry detection identifies components of magnetic discontinuity such as lithological boundaries, faults and dykes (these are positive features). This give rise to (Figure. 9) which is the structural map of the area.

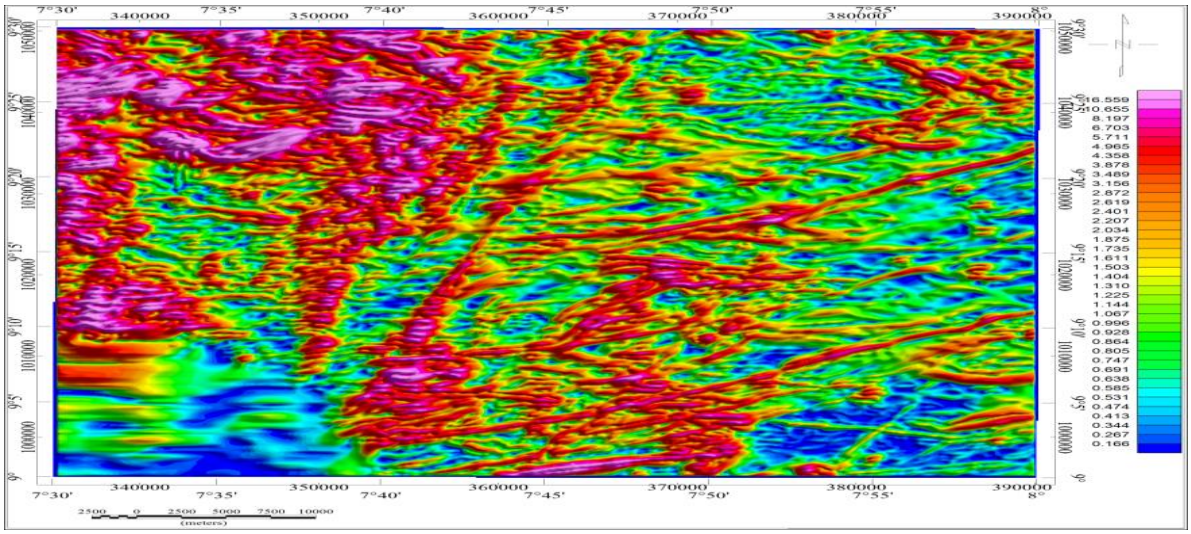

Figure: 7. Standard Deviation map (nT/m)

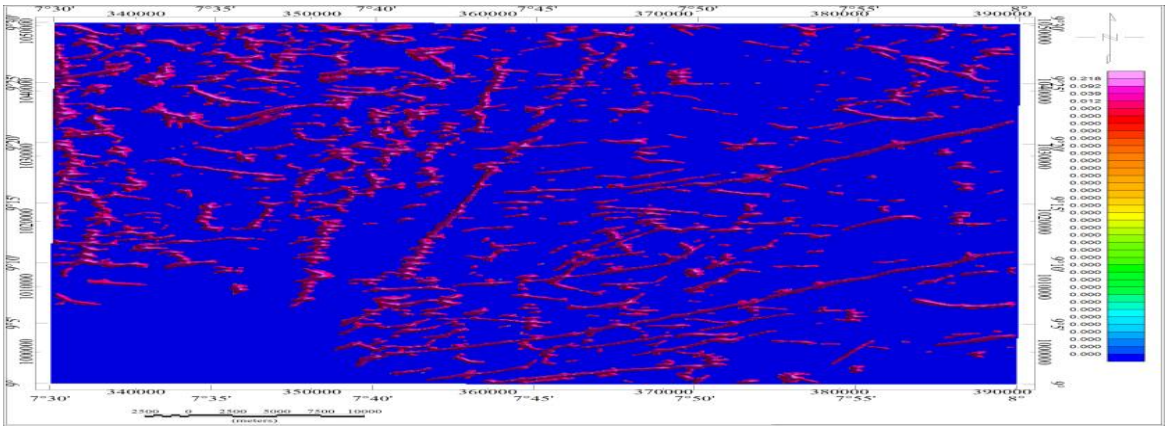

Figure: 8. Phase Symmetry Map

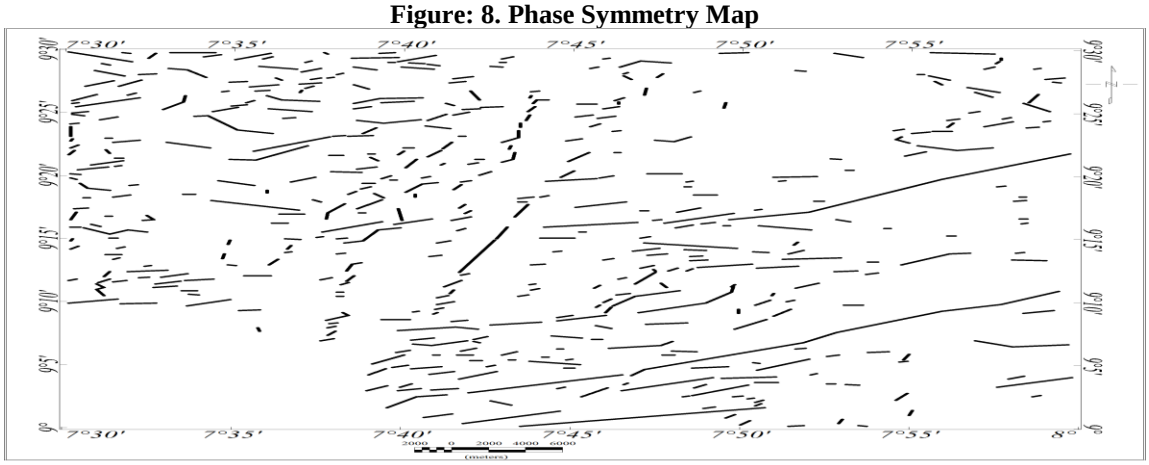

Figure: 9. Vectorise Structural (Lineament) Map of the area

3.4 Interpretation of 3D Euler Deconvolution

According to Reid *et al.*, (1990), magnetic contact has a structural index of zero; however, actual faults are usually complicated structures, and the use of slightly greater indices is often suitable. Therefore, the structural index of 1 was chosen in order to differentiate faults / fractures from lithological contacts in the study area. Figure.10 displays the Euler solution plot for the 1 structural index. The depths were divided or grouped at every 150 m and the result reveals that the faults / fractures between the depths of 150 and 300 m dominate the research area. The result also shows prominent NE–SW and NW–SE trending structures. A critical visual inspection of the faulting pattern indicated by the NE–SW trending alignments of many Euler solutions shows that the study area has been affected by an NE–SW trending regional fault system.

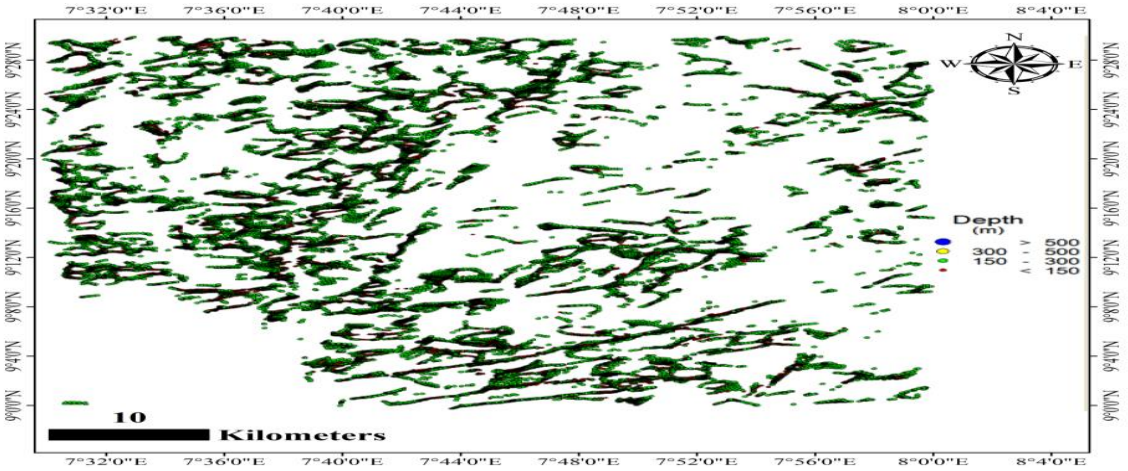

Figure.10. Euler solution map for a structural index (N) of 1

4.0 CONCLUSIONS

The HRAD was processed to identify anomalies of concern and Euler deconvolution obtained an estimate of depths between 150 m and 500 m. The analysis of the HRAD's first vertical derivative and CET revealed that the research area is highly faulted (Figure 6) and (Figure. 9). From the analysis of 3D Euler deconvolution, depths were divided or grouped at every 150 m and the result shows that the faults / fractures between the depths of 150 and 300 m dominate the research area (Figure 10). The outcome also reveals the prominent trending NE–SW and NW–SE structures within the study area. A critical visual inspection of the fault pattern indicated by the FVD, CET and NE–SW trend alignment of many Euler solutions indicates that the study area has been seriously influenced by the NE–SW trend of a regional fault system**.**

5.0 RECOMMENDATION

2-D Resistivity survey is highly recommended in this area of research as it will assist to define the depth of the structures identified from aeromagnetic data interpretation. Resistivity mapping can provide other important information in the study area and is significant because it can be used to identify weak areas and is useful for minimising hazards associated with unstable areas within the study area as the presence of major faults and fractures can lead to significant changes in resistivity values for a survey line, depth to structures (faults and fractures) can be established and thicknesses of overburden can also be delineated easily compared to aeromagnetic data interpretation.

REFERENCES

Azizi, M., Saibi, H.,& Cooper, G.R.J., (2015). Mineral and structural mapping of the Aynak-Logar Valley (Eastern Afghanistan) from hyperspectral remote sensing data and aeromagnetic data. ArabianJ. Geosciences 8, 10911e10918. https:// doi.org/10.1007/s12517-015-1993-2.

Baranov, V., (1957). A new method of interpretation of aeromagnetic maps: Pseudogravimetric anomalies. *Geophysics*.22. 259-283

Black, R. (1980). Precambrian of West Africa. Episodes 4:3–8

Core, D., Buckingham, A., & Belfield, S., (2009). Detailed structural analysis of magnetic data -done quickly and objectively, SGEG Newsletter.

Domzalski, W. (1966). Importance of aeromagnetics in evaluation of structural control of mineralization. *Geophysic*. Prospection. XIV (3), 273–291.

Farhi, W., Boudella, A., Saibi, H., &Bounif, M.O.A., (2016). Integration of magnetic, gravity, and well data in imaging subsurface geology in the KsarHirane region (Laghouat, Algeria). J. Afr. Earth Sci. 124, 63e74.

Foss, C. (2011). Magnetic data Enhancement and Depth Estimation. (H. Gupta, Ed.) Encyclopedia of Earth Sciences Series, 736-746.

Khashaba, A., Mekkawi, M., Ghamry, E.,& Abdel Aal, E., (2016). Land magnetic investigationon the west Qarun oil field, western Desert-Egypt. J. Geol. Geophys. 5,272. https://doi.org/10.4172/2381-8719.1000272.

Holden, E.J., Dentith, M., &Kovesi, P., (2008). Towards the automatic analysis of regional aeromagnetic data to identify regions prospective for gold deposits. Comput. Geosci.34, 1505–1513.

NGSA, (2006). Geology and Structural Lineament Map of Nigeria.

Reid, A. B., Allsop J. M., Granser, H., Mille,t A.J.,& Somerton IW (1990). Magnetic interpretation in three dimensions using Euler deconvolution. *Geophysics* 55:80–91

Thompson, D. T, (1982) EULDPH: a new technique for making computer-assisted depth estimates from magnetic data. Geophysics47:31–37

Yaoguo, L., & Douglas, W. O (2001,). Stable reduction to the pole at the magnetic equator*Geophysics*, VOL. 66(2); P. 571–578, 7